Ultrafast and selective coherent population transfer in four-level atoms by a single nonlinearly chirped femtosecond pulse

Parvendra Kumar and Amarendra K. Sarma[*]

Department of Physics, Indian Institute of Technology Guwahati, Guwahati-781039, Assam, India
(Received 8 June 2013; published 13 September 2013)

We report a simple scheme to achieve ultrafast and selective population transfer in four-level atoms by utilizing a single nonlinearly chirped femtosecond pulse. It is demonstrated that the almost complete population may be transferred to the preselected state of atoms just by manipulating the so-called frequency offset parameter. The robustness of the scheme against the variation of laser pulse parameters is also investigated. The proposed scheme may be useful for selective population transfer in molecules.

I. INTRODUCTION

The development of many efficient schemes such as stimulated Raman adiabatic passage (STIRAP), Raman chirped adiabatic passage (RCAP), and adiabatic rapid passage (ARP) for controlling the population transfer between the quantum states of atoms and molecules has opened new routes for controlling various atomic and molecular processes [1–10]. For example, coherent control is now conceived as a very useful method to actively influence the outcome of a chemical reaction [11–13]. Moreover, today coherent control techniques are widely used in the fields of robust quantum dot excitation generation [14], controllable coherent population transfer in superconducting qubits [15], collision dynamics [11,13], atomic interferometry [16,17], high precision spectroscopy [18,19], quantum computing [15,20,21], quantum information processing [22,23], and ultrafast optical switching [24–26]. Many authors have demonstrated selective and efficient population transfer to the target state by combining two or more schemes. For example, Band and Magnes [27] demonstrated selective coherent population transfer (CPT) in Λ-like or ladderlike four-level atoms by combining STIRAP and RCAP techniques. Moreover, Yang and Zhu [28] investigated the effect of collisions on control of CPT in inverse Y-type four-level atoms driven by three laser fields with the STIRAP scheme. They found that low population transfer efficiency could be enhanced dramatically with an increase of collision-induced coherence decay rates. In another study, Yang *et al.* [29] presented an efficient scheme for selective CPT in Λ-like four-level atoms by combining STIRAP, temporal coherent control (TCC), and RCAP techniques. Apart from the coherent control of population transfer using two or more pulses, recently much attention has been paid towards realizing CPT by using a single frequency chirped pulse in three- and four-level atoms, owing to the easy realization of complete population transfer. In particular, Djotyan *et al.* [30] demonstrated CPT in Λ-like atoms using a single frequency-chirped laser pulse. Very recently, Collins and Malinovskaya [19] demonstrated CPT in Λ-like three-level rubidium atoms with a low-intensity chirped pulse. Again, Zhang *et al.* [31] have proposed a scheme for CPT and arbitrary superpositions of quantum states by a single-chirped laser pulse in a Λ-like excited-doublet

four-level system. They demonstrated efficient and robust CPT via a single-chirped pulse when the pulse bandwidth is smaller than about $1/10$ of the energy separation between the excited-doublet levels and between the ground states. In the present article, we discuss and demonstrate a scheme for selective and ultrafast CPT in a system of Y-like four-level Na atoms by using a nonlinearly chirped femtosecond laser pulse. It is shown that selective CPT could be achieved simply by manipulating the frequency offset parameter, defined later in the article. The phenomenon of CPT is investigated by numerically solving the appropriate density matrix equations beyond the rotating wave approximation. In addition, we assume that all the atomic relaxation times are considerably longer than the interaction times. In Sec. II we present the optical Bloch equations that describe the interaction of the Y-like four-level system with a single femtosecond laser pulse. Section III contains our simulated results and discussions, followed by conclusions in Sec. IV.

II. THE MODEL

Our proposed scheme is depicted in Fig. 1. In Fig. 1, the levels $|1\rangle, |2\rangle, |3\rangle$, and $|4\rangle$ represent the $3s$, $3p$, $5s$, and $4d$ states of the sodium atom, respectively. The complete Hamiltonian, without invoking the rotating wave approximation, which describes the interaction of a single pulse with four-level atoms, is given by

$$\hat{H} = \hbar \begin{pmatrix} \omega_1 & -\Omega_{12}(t) & 0 & 0 \\ -\Omega_{12}(t) & \omega_2 & -\beta\Omega_{12}(t) & -\gamma\Omega_{12}(t) \\ 0 & -\beta\Omega_{12}(t) & \omega_3 & 0 \\ 0 & -\gamma\Omega_{12}(t) & 0 & \omega_4 \end{pmatrix}.$$

$$(1)$$

Here, $\Omega_{12}(t) = \mu_{12}E(t)/\hbar$ is the time-dependent Rabi frequency and μ_{12} is the transition dipole moment of the $|1\rangle \rightarrow |2\rangle$ transition. The transition dipole moments μ_{23} and μ_{24} are chosen as follows: $\mu_{23} = \beta\mu_{12}$ and $\mu_{24} = \gamma\mu_{12}$. Here, β and γ are the dipole moment coefficients. The electric field part of the pulse is defined as follows: $E(t) = f(t)\cos[\omega t + \delta(t)]$, where $f(t)$ is the pulse envelope, given by $f(t) = E_0\exp[-(t/\tau_p)^2]$. Here, E_0 is the peak amplitude of the pulse envelope, $\tau_{\text{FWHM}} = 1.177\tau_{p,\omega}$ is the central frequency, and $\delta(t)$ is the time-varying
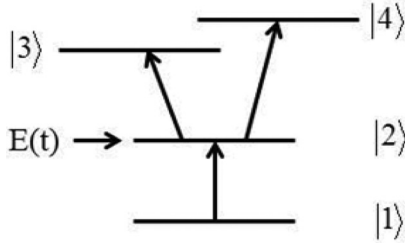
———————
[*]aksarma@iitg.ernet.in

FIG. 1. Schematic of the scheme.

phase, say, the chirping parameter. The temporal profile of $\delta(t)$ is defined as $\delta(t) = -\alpha \tanh[(t - t_0)/\tau]$. This temporal profile has been considered by other researchers as well as in various contexts [32,33]. The chirping parameter of the pulse may be controlled by manipulating the three parameters α, t_0, and τ. In this work, these three control parameters are termed as the frequency sweeping, the frequency offset, and the frequency steepening parameters, respectively. The time-varying frequency of the pulse has the form $\omega(t) = \omega - \alpha \operatorname{sech}^2[(t - t_0)/\tau]/\tau$. The Bloch equations, without invoking the so-called rotating wave approximation, describing the temporal evolution of the density matrix elements, are

$$\frac{d\rho_{11}}{dt} = i\Omega_{12}(t)(\rho_{21} - \rho_{12}),$$

$$\frac{d\rho_{22}}{dt} = i\Omega_{12}(t)[\rho_{12} - \rho_{21} + \beta(\rho_{32} - \rho_{23}) + \gamma(\rho_{42} - \rho_{24})],$$

$$\frac{d\rho_{33}}{dt} = i\Omega_{12}(t)[\beta(\rho_{23} - \rho_{32})],$$

$$\frac{d\rho_{44}}{dt} = i\Omega_{12}(t)[\gamma(\rho_{24} - \rho_{42})],$$

$$\frac{d\rho_{43}}{dt} = -i\omega_{43}\rho_{43} + i\Omega_{12}(t)(\gamma\rho_{23} - \beta\rho_{42}),$$

$$\frac{d\rho_{42}}{dt} = -i\omega_{42}\rho_{42} + i\Omega_{12}(t)[\gamma(\rho_{22} - \rho_{44}) - \rho_{41} - \beta\rho_{43}],$$

$$\frac{d\rho_{41}}{dt} = -i\omega_{41}\rho_{41} + i\Omega_{12}(t)(\gamma\rho_{21} - \rho_{42}),$$

$$\frac{d\rho_{32}}{dt} = -i\omega_{32}\rho_{32} + i\Omega_{12}(t)[\beta(\rho_{22} - \rho_{33}) - \rho_{31} - \gamma\rho_{34}],$$

$$\frac{d\rho_{31}}{dt} = -i\omega_{31}\rho_{31} + i\Omega_{12}(t)(\beta\rho_{21} - \rho_{32}),$$

$$\frac{d\rho_{21}}{dt} = -i\omega_{21}\rho_{21} + i\Omega_{12}(t)(\rho_{11} - \rho_{22} + \beta\rho_{31} + \gamma\rho_{41}). \quad (2)$$

Here $\omega_{ij} = \omega_i - \omega_j$. It may be noted that $\rho_{ij} = \rho_{ji}^*$. $\rho_{nm}(n, m = 1 \to 4)$ is the component of the density matrix, ρ_{nn} is related to the population of the nth level, while ρ_{nm} refers to the coherence between the n level and the m level. The time-independent Rabi frequencies are defined as follows: $\Omega_{12} = \mu_{12}E_0/\hbar$, $\Omega_{23} = \mu_{23}E_0/\hbar = \beta\Omega_{21}$, and $\Omega_{24} = \mu_{24}E_0/\hbar = \gamma\Omega_{21}$. We use the following typical parameters: $\Omega_{12} = 0.60$ rad/fs, $\omega_{21} = 3.19$ rad/fs, $\omega_{32} = 3.06$ rad/fs, $\omega_{42} = 3.30$ rad/fs, $\tau_p = 16.5$ fs, $t_0 = \mp16.5$ fs, $\tau = 16.5$ fs, $\omega = 3.6$ rad/fs, $\beta = 0.90$, $\gamma = 1.10$, and $\alpha = 10.0$ rad. It is worth mentioning that the aforementioned pulse parameters are chosen so that selective and maximum population transfer could be achieved.

III. RESULTS AND DISCUSSIONS

In Fig. 2, the effects of the variation of the control parameters on the time-varying pulse frequency are depicted. Figure 2(a) depicts the temporal evolution of the pulse frequency for control parameters $\alpha = 10.0$ rad, $t_0 = -16.5$ fs, and $\tau = 16.5$ fs. It is observed that with $\alpha = 10.0$ rad, the sweeping of pulse frequency occurs from 3.6 to 3.0 rad/fs. The dip in the time-varying frequency occurs at time $t = -16.5$ fs, which is equal to the frequency offset parameter $t_0 = -16.5$ fs. It should be noted that for the chosen pulse
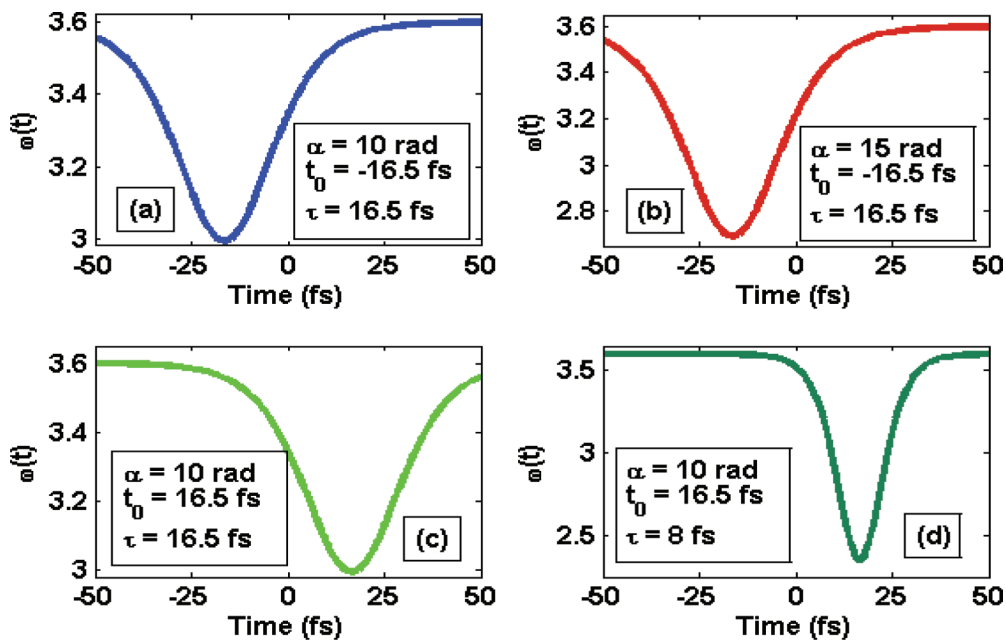

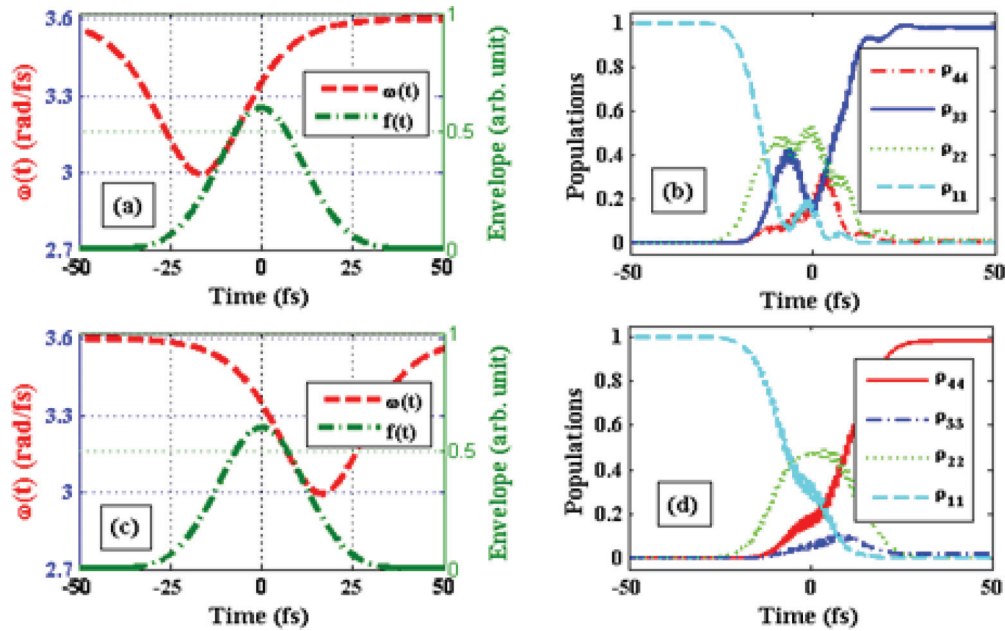FIG. 2. (Color online) Temporal evolution of the pulse frequency.

FIG. 3. (Color online) Temporal evolution of the pulse frequency [(a), (c)], the pulse envelope [(a), (c)], and the populations [(b), (d)].

parameters ($\alpha = 10.0$ rad, $\tau = 16.5$ fs) the frequency spectrum of the nonlinearly chirped pulse overlaps with the transition frequencies of the chosen states of a real sodium atom. On the other hand, transitions between the other states are either off resonant or dipole forbidden. However, the same frequency sweeping range (3.6–3.0 rad/fs) may be achieved also for other parameters (e.g., $\alpha = 14$ and $\tau = 24$). In Fig. 2(b), the result is plotted for a different frequency sweeping parameter α while keeping the other parameters unchanged. It can be observed from Fig. 2(b) that with $\alpha = 15$ rad, the sweeping of pulse frequency occurs from 3.6 to 2.5 rad/fs. It can be seen from Fig. 2(c) that the dip in the time-varying frequency occurs at time $t = 16.5$ fs, which is equal to the frequency offset parameters $t_0 = 16.5$ fs. Hence, the frequency offset parameter is responsible for the shifting of the temporal position of the dip in the time-varying frequency. In Fig. 2(d), we have changed the frequency steepening parameter τ, keeping the other parameters the same as those in Fig. 2(c), in order to examine the effect of the τ parameter on the time-varying frequency. It is observed that for the frequency steepening parameter $\tau = 8$ fs, along with the sweeping, the steepening of the temporal profile of the pulse frequency also occurs. It is clear that the temporal profile of the phase considered in this work offers the possibility to select a particular transition path if the control parameters are chosen judiciously. Next, in Fig. 3, we depict the temporal evolution of the pulse frequency, the pulse envelope, and the populations in different states. The control parameters chosen here are $\alpha = 10$ rad and $\tau = 16.5$ fs. On the other hand, the frequency offset parameter chosen is $t_0 = -16.5$ fs in Figs. 3(a) and 3(b) and $t_0 = 16.5$ fs in Figs. 3(c) and 3(d).

It may be understood from Fig. 3(a) that the pulse is interacting with the $|1\rangle \rightarrow |2\rangle$ and $|2\rangle \rightarrow |3\rangle$ transitions in a counterintuitive manner because with the chosen frequency offset parameter, $t_0 = -16.5$ fs, initially the time-varying frequency is resonant with the $|2\rangle \rightarrow |3\rangle$ transition frequency

at time $t \approx -18$ fs, and at a later time $t \approx -8$ fs, it is resonant with the $|1\rangle \rightarrow |2\rangle$ transition frequency. This counterintuitive sequence makes the $|2\rangle \rightarrow |4\rangle$ transition nearly forbidden and leads to almost complete (98.40%) population transfer to state $|3\rangle$, as can be observed in Fig. 3(b). On the other hand, it might be clear from Fig. 3(c) that the pulse is interacting with the $|1\rangle \rightarrow |2\rangle$ and $|2\rangle \rightarrow |4\rangle$ transitions in a counterintuitive manner also, because, with the chosen frequency offset parameter $t_0 = 16.5$ fs, initially the time-varying frequency is resonant with the $|2\rangle \rightarrow |4\rangle$ transition frequency at $t \approx 2$ fs, while at a later time $t \approx 6$ fs, it is resonant with the $|1\rangle \rightarrow |2\rangle$ transition frequency. This counterintuitive sequence makes the $|2\rangle \rightarrow |3\rangle$ transition nearly forbidden
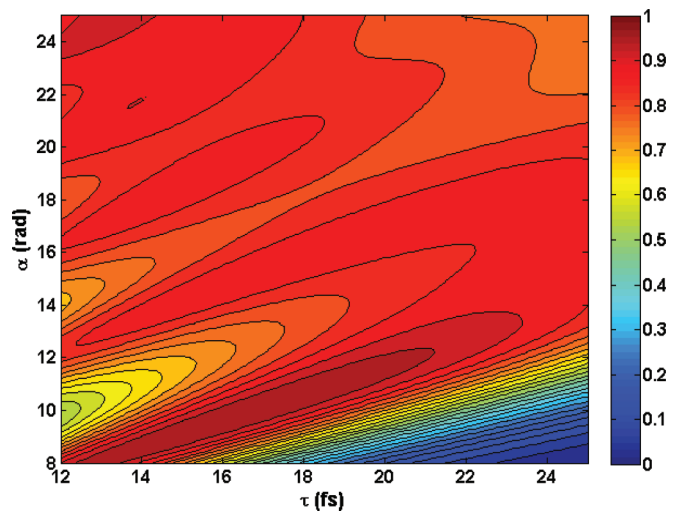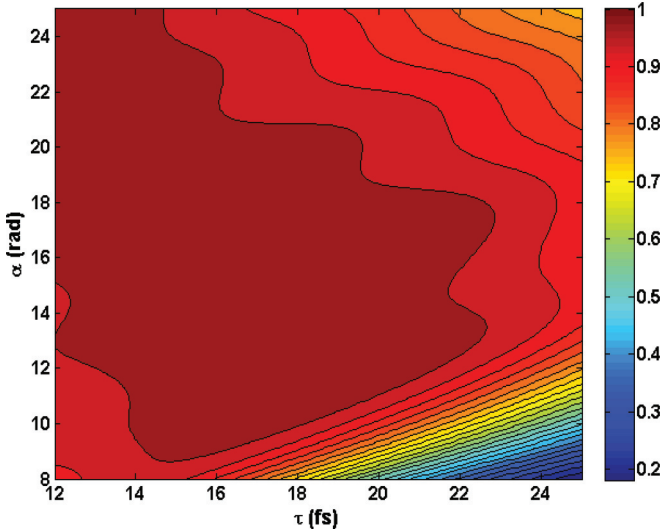

FIG. 4. (Color online) Contour plots of the final population $\rho_{33}(\infty)$ for the varying frequency sweeping parameter α and the frequency steepening parameter τ. Other parameters are the same as in Fig. 3(a).

FIG. 5. (Color online) Contour plots of the final population $\rho_{44}(\infty)$ for the varying frequency sweeping parameter α and the frequency steepening parameter τ. Other parameters are the same as in Fig. 3(c).

FIG. 7. (Color online) Contour plots of the final population $\rho_{33}(\infty)$ for the varying Rabi frequency Ω_{12} and pulse width τ_{FWHM}. Other parameters are the same as in Fig. 3(a).

and leads to almost complete (98.50%) population transfer to state $|4\rangle$, as can be observed in Fig. 3(d). Hence selective population transfer could be achieved just by manipulating the chirp offset parameter. It is important to verify the robustness of the scheme against the variation of the pulse parameters for practical realization of the scheme. So, in Figs. 4 and 5, we present the simulation result for the variation of the final population transfer to state $|3\rangle$, i.e., $\rho_{33}(\infty)$, and state $|4\rangle$, i.e., $\rho_{44}(\infty)$, with frequency sweeping and frequency steepening parameters.

A careful inspection of Fig. 4 reveals that the final population in state $|3\rangle$, $\rho_{33}(\infty)$, is fairly robust against a small variation in the frequency sweeping parameter α and the frequency steepening parameter τ. One can obtain a more than 95% population transfer against the variation in these parameters in the range, say, $\alpha \approx 8$–11 rad and $\tau \approx 12.5$–21 fs. However, a more than 85% population transfer is possible in a sufficiently large range of variation in α and τ.

Figure 5 reveals that the final population in state $|4\rangle$, $\rho_{44}(\infty)$, is sufficiently robust against variation in the
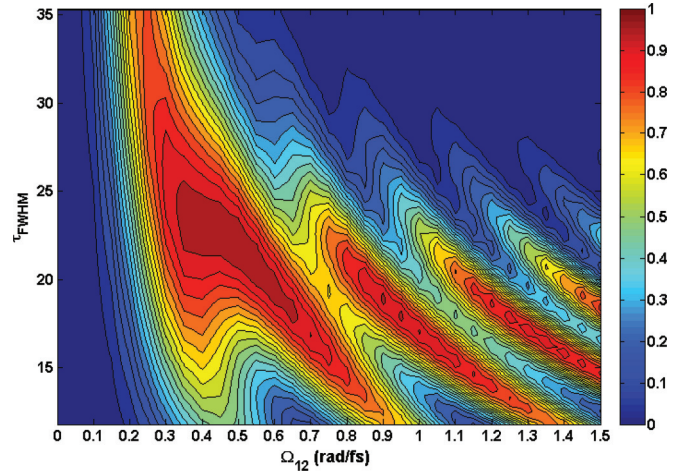
frequency sweeping parameter α and the frequency steepening parameter τ to a large range, $\alpha \approx 9$–25 rad and $\tau \approx 12$–22 fs, respectively, which amounts to more than 95% population. Thus the final population transfer to state $|4\rangle$ is more robust compared to that of the final population transfer to state $|3\rangle$. For example, one can obtain a nearly 67% population transfer to state $|3\rangle$ with $\alpha = 11$ rad and $\tau = 14$ fs, as can be observed in Fig. 4, while with the same set of control parameters one can obtain a nearly 97% population transfer to state $|4\rangle$, as can be observed in Fig. 5. In order to investigate the reason behind this difference, we depict the temporal evolution of the time-varying pulse frequency and pulse envelope in Fig. 6.

It can be observed from Fig. 6(a) that the time-varying frequency $\omega(t)$ with $\alpha = 11$ rad, $t_0 = -16.5$ fs, and $\tau = 14$ fs is resonant with the frequency of the $|2\rangle \rightarrow |3\rangle$ transition at time $t \approx -24.4$ fs. At a later time $t \approx -4.7$ fs, it is resonant with the frequency of the $|1\rangle \rightarrow |2\rangle$ transition. It can be seen that at time $t = -24.4$ fs, the corresponding value of the pulse envelope is too low (0.04) to completely transfer population to state $|3\rangle$, while the pulse envelope has a value (0.25) at time $t = -18$ fs [see Fig. 3(a)]. However, the time-varying frequency $\omega(t)$ with $\alpha = 11$ rad, $t_0 = 16.5$ fs, and $\tau = 14$ fs is resonant with the frequency of the $|2\rangle \rightarrow |4\rangle$ transition at time
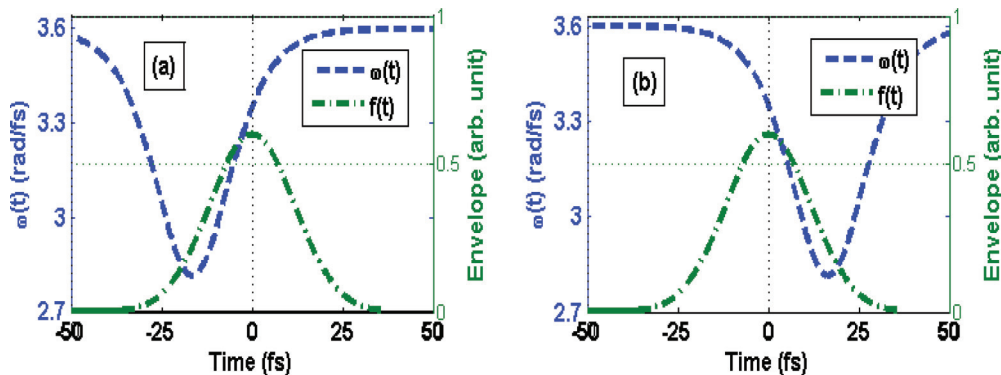

FIG. 6. (Color online) Temporal evolution of the pulse frequency $\omega(t)$ and the pulse envelope $f(t)$: (a) $\alpha = 11$ rad, $t_0 = -16.5$ fs, and $\tau = 14$ fs; (b) $\alpha = 11$ rad, $t_0 = 16.5$ fs, and $\tau = 14$ fs.
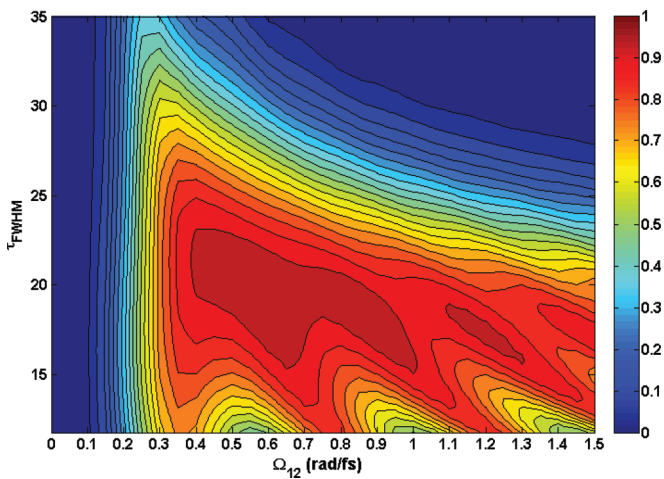
FIG. 8. (Color online) Contour plots of the final population $\rho_{44}(\infty)$ for the varying Rabi frequency Ω_{12} and pulse width τ_{FWHM}. Other parameters are the same as in Fig. 3(c).

$t \approx 1.65$ fs, and at a later time $t \approx 25.7$ fs it is resonant with the frequency of the $|1\rangle \rightarrow |2\rangle$ transition. It could be seen that at time $t = 1.65$ fs the corresponding value of the pulse envelope is sufficient (0.59) to transfer nearly all of the population to state $|4\rangle$, which is nearly equal to the pulse envelope value (0.58) at time $t = 2$ fs, as can be seen from Fig. 3(c). In Fig. 7, we depict the robustness of the final population transfer to state $|3\rangle$ with respect to the pulse duration and the time-independent Rabi frequency. It can be seen that $\rho_{33}(\infty)$ is fairly robust against variation in the pulse duration and the time-independent Rabi frequency in the range $\tau_{\text{FWHM}} = 21$–26 fs and $\Omega_{12} = 0.35$–0.55 rad/fs, respectively.

In Fig. 8, we depict the robustness of the final population transfer to state $|4\rangle$ with respect to the pulse duration τ_{FWHM} and the time-independent Rabi frequency Ω_{12}. It can be observed from Fig. 8 that $\rho_{44}(\infty)$ is fairly robust against the variation in the pulse duration and the time-independent Rabi frequency in the range $\tau_{\text{FWHM}} = 16$–22 fs and $\Omega_{12} = 0.4$–1.0 rad/fs, respectively. In addition, $\rho_{33}(\infty)$ and $\rho_{44}(\infty)$ are

found to be nearly 96% and 97%, respectively, for $\beta = \gamma = 1$ and nearly 92% each for $\beta = 1.1$ and $\gamma = 0.9$. However, one can achieve more than 92% population with $\beta = 1.1$ and $\gamma = 0.9$ by judiciously choosing the pulse parameters such as Ω_{12}, α, and τ. For example, nearly 97% population transfers to state $|3\rangle$ may be achieved with $\Omega_{12} = 0.55$ rad/fs, $\alpha = 11.50$ rad, and $\tau = 18$ fs.

IV. CONCLUSIONS

In Y-like four-state Na atoms, we have demonstrated ultrafast and selective population transfer using a single nonlinearly chirped femtosecond pulse. Effects of the control parameters on the temporal phase have been investigated. We have suggested that by judicious choice of the control parameters, one can select the specific transitions states of an atom. We have demonstrated selective coherent population transfer either to the third or fourth state by manipulating the frequency offset parameter. Selective population transfer is found to be robust against variations in the simulation parameters such as the time-independent Rabi frequency, the frequency sweeping parameter, the frequency steepening parameter, and the dipole moment coefficients. This scheme may be explored in other atoms as well which could be modeled as Y-like four-level atoms such as lithium, potassium, and rubidium. The scheme may also be explored in the electronic states of molecules owing to the selectivity offered by the frequency offset parameter. For example, the proposed scheme may be explored in the electronic states ($X\,^1\sum_g^+$, $A\,^1\sum_u^+$, $1\,^1\Pi_g$, and $2\,^1\Pi_g$) [34,35] of sodium molecules. Here, the electronic states $X\,^1\sum_g^+$, $A\,^1\sum_u^+$, $1\,^1\Pi_g$, and $2\,^1\Pi_g$ denote the quantum states $|1\rangle$, $|2\rangle$, $|3\rangle$, and $|4\rangle$ of the chosen atomic system, respectively.

[1] N. V. Vitanov, T. Halfmann, B. W. Shore, and K. Bergmann, Annu. Rev. Phys. Chem. **52**, 763 (2001).

[2] B. W. Shore, *The Theory of Coherent Atomic Excitation* (Wiley, New York, 1990).

[3] W.-T. Liao, A. Pálffy, and C. H. Keitel, Phys. Lett. B **705**, 134 (2011).

[4] P. Lambropoulos and D. Petrosyan, *Fundamentals of Quantum Optics and Quantum Information* (Springer, Berlin, 2007).

[5] D. Yan, C.-L. Cui, M. Zhang, and J.-H. Wu, Phys. Rev. A **84**, 043405 (2011).

[6] H. Maeda, J. H. Gurian, D. V. L. Norum, and T. F. Gallagher, Phys. Rev. Lett. **96**, 073002 (2006).

[7] M. M. Martin and J. T. Hynes, *Femtochemistry and Femtobiology: Ultrafast Events in Molecular Science* (Elsevier, Amsterdam, 2004).

[8] M. Shapiro and P. Brumer, *Quantum Control of Molecular Processes* (Wiley-VCH, Weinheim, 2012).

[9] M. Oberst, H. Münch, and T. Halfmann, Phys. Rev. Lett. **99**, 173001 (2007).

[10] B. D. Fainberg and V. A. Gorbunov, J. Chem. Phys. **117**, 7222 (2002).

[11] M. Külz, M. Keil, A. Kortyna, B. Schellhaass, J. Hauck, K. Bergmann, W. Meyer, and D. Weyh, Phys. Rev. A **53**, 3324 (1996).

[12] P. Dittmann, F. P. Pesl, J. Martin, G. W. Coulston, G. Z. He, and K. Bergmann, J. Chem. Phys. **97**, 9472 (1992).

[13] Y. Ohta, K. Hoki, and Y. Fujimura, J. Chem. Phys. **116**, 7509 (2002).

[14] C. M. Simon, T. Belhadj, B. Chatel, T. Amand, P. Renucci, A. Lemaitre, O. Krebs, P. A. Dalgarno, R. J. Warburton, X. Marie, and B. Urbaszek, Phys. Rev. Lett. **106**, 166801 (2011).

[15] L. F. Wei, J. R. Johansson, L. X. Cen, S. Ashhab, and F. Nori, Phys. Rev. Lett. **100**, 113601 (2008).

[16] L. S. Goldner, C. Gerz, R. J. C. Spreeuw, S. L. Rolston, C. I. Westbrook, W. D. Phillips, P. Marte, and P. Zoller, Phys. Rev. Lett. **72**, 997 (1994).

[17] J. Lawall and M. Prentiss, Phys. Rev. Lett. **72**, 993 (1994).

[18] R. Sussmann, R. Neuhauser, and H. Neusser, J. Chem. Phys. **100**, 4784 (1994).

[19] T. A. Collins and S. A. Malinovskaya, Opt. Lett. **37**, 2298 (2012).

[20] D. Møller, L. B. Madsen, and K. Mølmer, Phys. Rev. Lett. **100**, 170504 (2008).

[21] J. L. Sørensen, D. Møller, T. Iversen, J. B. Thomsen, F. Jensen, P. Staanum, D. Voigt, and M. Drewsen, New J. Phys. **8**, 261 (2006).

[22] T. Beth and G. Leuchs, *Quantum Information Processing* (Wiley-VCH, Weinheim, 2005).

[23] M. Saffman and T. G. Walker, Rev. Mod. Phys. **82**, 2313 (2010).

[24] H. Suchowski, Y. Silberberg, and D. B. Uskov, Phys. Rev. A **84**, 013414 (2011).

[25] C. Y. Ye, V. A. Sautenkov, Y. V. Rostovtsev, and M. O. Scully, Opt. Lett. **28**, 2213 (2003).

[26] P. Kumar and A. K. Sarma, Phys. Rev. A **87**, 025401 (2013).

[27] Y. B. Band and O. Magnes, Phys. Rev. A **50**, 584 (1994).

[28] X. Yang and S. Zhu, Phys. Rev. A **78**, 023818 (2008).

[29] X. Yang, Z. Zhang, X. Yan, and C. Li, Phys. Rev. A **81**, 035801 (2010).

[30] G. P. Djotyan, J. S. Bakos, Zs. Sörlei, and J. Szigeti, Phys. Rev. A **70**, 063406 (2004).

[31] Z. Zhang, X. Yang, and X. Yan, J. Opt. Soc. Am. B **30**, 1017 (2013).

[32] N. Cui, Y. Xiang, Y. Niu, and S. Gong, New J. Phys. **12**, 013009 (2010).

[33] J. J. Carrera and S.-I Chu, Phys. Rev. A **75**, 033807 (2007).

[34] B. M. Garraway and K.-A. Suominen, Phys. Rev. Lett. **80**, 932 (1998).

[35] I. R. Solá, B. Y. Chang, J. Santamaría, V. S. Malinovsky, and J. L. Krause, Phys. Rev. Lett. **85**, 4241 (2000).